

# Cysteine Biosynthetic Enzymes Are the Pieces of a Metabolic Energy Pump<sup>†</sup>

Jiang Wei, Qing-Xiu Tang, Olga Varlamova, Camille Roche, Reaching Lee, and Thomas S. Leyh\*

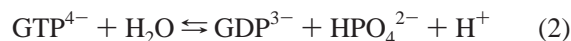
The Department of Biochemistry, Albert Einstein College of Medicine, 1300 Morris Park Avenue, Bronx, New York 10461-1926

Received April 12, 2002; Revised Manuscript Received May 9, 2002

**ABSTRACT:** Understanding the mechanisms of free energy transfer in metabolism is fundamental to understanding how the chemical forces that sustain the molecular organization of the cell are distributed. Recent studies of molecular motors (1–3) and ATP-driven proton transport (4–6) describe how chemical potential is transferred at the molecular level. These systems catalyze energy transfer through structural change and appear to be dedicated exclusively to their coupling tasks (7, 8). Here we report the discovery of a new class of energy-transfer system. It is a biosynthetic pump composed of cysteine biosynthesis enzymes, ATP sulfurylase and *O*-acetylserine sulfhydrylase, each with its own catalytic function and from whose interactions emerge *new* function: the hydrolysis of ATP. The hydrolysis is kinetically and energetically linked to the chemistry catalyzed by ATP sulfurylase, the first enzyme in the cysteine biosynthetic pathway, in such a way that each molecule of ATP hydrolyzed, each stroke of the pump, produces 1 equivalent of that enzyme's product. These findings integrate cysteine metabolism and broaden our understanding of the ways in which higher order allostery is used to effect free energy transfer.

Entry of sulfate into sulfur metabolism requires that it be chemically activated. Activation is achieved by transferring the adenylyl moiety (~AMP) of ATP from pyrophosphate to sulfate to form adenosine 5'-phosphosulfate (i.e., activated sulfate, or APS) (reaction 1). The remarkably high energy of the phosphoric–sulfuric acid anhydride formed in this transfer ( $\Delta G_{\text{hydrolysis}}^{\circ} \sim -19$  kcal/mol) enables sulfate, which is otherwise nonreactive, to participate in its subsequent metabolic biochemistry. Under presumed near-physiological conditions, the synthesis of APS is extremely unfavorable ( $K_{\text{eq}} = 1.1 \times 10^{-8}$ ) despite cleavage of the  $\alpha,\beta$ -bond of ATP (9). Cells that must acquire nutrients against such unfavorable equilibria are faced with a mass action problem, and a kinetic problem due to the fact that the catalyst will be less efficient in the unfavorable direction by a factor equal to the reaction's equilibrium constant, in this case,  $1.1 \times 10^8$ -fold less efficient. The data presented in this paper suggest that *Escherichia coli* K-12 overcomes these problems by assembling a multifunctional protein complex using the cysteine biosynthetic enzymes: ATP sulfurylase and *O*-acetylserine sulfhydrylase (10, 11).

The biosynthetic enzymes in question are the first and last enzymes in the cysteine biosynthetic pathway in *E. coli* K-12: ATP sulfurylase and *O*-acetylserine sulfhydrylase (OASS) (10, 11). ATP sulfurylase is a complex enzyme. It is a tetramer of heterodimers, each composed of an APS synthesis and a GTPase subunit, which catalyze reactions 1 and 2, respectively (12). The GTPase- and APS-forming reactions are coupled by allosteric interactions that occur during the catalytic cycle; however, the enzyme does not require GTP to catalyze APS synthesis (13). Activated sulfate is an ancient, high-energy metabolite that serves several



cellular functions (14). It is the immediate precursor of PAPS (3'-phosphoadenosine 5'-phosphosulfate), the universal sulfuryl group donor. Sulfuryl transfer, much like phosphoryl transfer, regulates the activities of a diverse group of metabolites including steroid and peptide hormones (15–17), neurotransmitters (18), and carbohydrate recognition determinants (19, 20). OASS, a homodimer, is structurally and functionally well characterized (21, 22). It catalyzes a pyridoxal 5'-phosphate-dependent  $\beta$ -elimination reaction in which acetate is displaced from *O*-acetyl-L-serine by hydrogen sulfide to form L-cysteine (reaction 3).



## MATERIALS AND METHODS

**Materials.** The materials and suppliers used in the study are as follows: restriction enzymes (New England Biolabs); Pfu polymerase, BL21-CodonPlus(DE3)-RIL (Stratagene); Superdex 200 prep grade, Sephacryl-300, hydroxylapatite, pyruvate kinase (rabbit muscle), and lactate dehydrogenase (rabbit muscle) (Pharmacia); Ni-NTA column (Qiagen); PEI-F<sup>1</sup> TLC plates (EM Science), DNA primers (Oligonucleotide Synthesis Facility, Albert Einstein College of Medicine); BL21(DE3) *E. coli* K-12, pET-23A expression vector (Novagen); inorganic pyrophosphatase (yeast), Sephadex G-100,  $\omega$ -aminohexylagarose, nucleotides, pyridoxine, thiamin, NAD<sup>+</sup>, pyrophosphate, IPTG, streptomycin, buffers,

<sup>†</sup> Supported by National Institutes of Health Grant GM54469.

\* Corresponding author. Phone: 718-430-2857. Fax: 718-430-8565. E-mail: leyh@aecom.yu.edu.

<sup>1</sup> Abbreviations: EDTA, ethylenediamine-*N,N,N',N'*-tetraacetic acid; PEI-F, poly(ethylenimine)–cellulose F; PMSF, phenylmethanesulfonyl fluoride; unit, micromoles of substrate converted to product per minute at  $V_{\text{max}}$ .

and salts (Sigma Chemical Co.); AX 300 HPLC column (SynChropak); Protein and Peptide C-18 (Vydac); [ $^{35}\text{S}$ ]SO $_4$  (ICN Pharmaceuticals); [ $\alpha$ - $^{32}\text{P}$ ]ATP (NEN Life Sciences Products). APS kinase from *E. coli* K-12 was purified as described previously (23). APS was synthesized and purified as described previously (24). JM83 is available from the American Type Culture Collection (25). GMPPNP (Roche Diagnostics) was purified to >95% using anion-exchange chromatography and a triethylamine/HCO $_3^-$  gradient (12).

**ATP Sulfurylase.** ATP sulfurylase, cloned from and expressed in *E. coli* K-12, was purified to >95% homogeneity using established protocols (26).

**Preparation of Extract for S-300 Chromatography (Figure 1).** Extract was prepared from 1 L of the *E. coli* K-12 strain JM83 (25) containing PGP1-2 (27) and pTL1, a plasmid that overexpresses ATP sulfurylase and APS kinase from *E. coli* K-12 (26). The cysteine biosynthetic enzymes were derepressed by growing the cells in VB (28) medium, in which SO $_4$  is the only source of sulfur, and by the addition of the inductant *O*-acetyl-L-serine (29), which was added at an OD $_{550}$  = 0.4. Cells were harvested at OD $_{550}$  = 1.0 by centrifugation and suspended in 4.0 mL/g wet weight in Tris-HCl (50 mM, pH = 8.0), KCl (100 mM), 2-mercaptoethanol (12 mM), glycerol (10% v/v), Na $_4$ EDTA (1.0 mM), pepstatin (0.1 mM), and PMSF (0.5 mM),  $T$  = 4 ( $\pm$  2)  $^\circ\text{C}$ . The suspended cells were lysed by sonication, and debris was removed by centrifugation at 4 ( $\pm$  2)  $^\circ\text{C}$ . The supernatant/extract (2.5 mL) was used in the experiment associated with Figure 1.

**Heat and Protease Inactivation of the Factor.** Four 1.5  $\mu\text{L}$  aliquots of trypsin (0.3 unit/ $\mu\text{L}$ ) or chymotrypsin (0.27 unit/ $\mu\text{L}$ ) were added to 30  $\mu\text{L}$  of partially purified factor (0.6 mg/mL) at three successive 1 h intervals. The reactions were run in Hepes (50 mM, pH = 8.0),  $T$  = 25 ( $\pm$  2)  $^\circ\text{C}$ . Following the final addition of protease, the reactions were run overnight, after which the proteolysis appeared complete by SDS-PAGE. Aprotinin, a protease inhibitor, was added to 27  $\mu\text{M}$ , and the proteolyzed factor was assayed for ATP sulfurylase activation using the assay described below (see, Figure 1: The APS Synthesis Assay) except for the following changes—ATP sulfurylase (17  $\mu\text{M}$ ), [ $^{35}\text{S}$ ]SO $_4$  (0.5 mM, SA = 4.7 Ci/mol), ATP/K $^+$  (1.0 mM), and MgCl $_2$  (2.1 mM). Control reactions were run to ensure that the nonproteolyzed factor was stable overnight, that aprotinin alone did not affect the factor-mediated activation of ATP sulfurylase, and that aprotinin protected ATP sulfurylase from protease inactivation.

The temperature stability of the factor was tested by incubating an extract prepared from *E. coli* K-12 strain 594 grown in VB medium (25 mg/mL) at 65 ( $\pm$  2)  $^\circ\text{C}$  for a defined time period, chilling the extract in an ice-water bath, and testing its ability to activate purified ATP sulfurylase using the assay described in the preceding paragraph. The extract was unable to activate ATP sulfurylase after 5 min at 65 ( $\pm$  2)  $^\circ\text{C}$ .

**Purification of the Factor from Wild-Type *E. coli* K-12.** Cell extract was prepared from the pellet of a 180 L growth of the *E. coli* strain DBan 594 (30) harvested in late-log phase from a minimal medium (28). The factor was purified to homogeneity using the following 11 consecutive steps: (1) streptomycin precipitation, (2) 40–65% ammonium sulfate cut, chromatography using the following matrices: (3)

Sephacryl S-300, (4) hydroxylapatite, (5) Sephadex G-100, (6)  $\omega$ -aminohexylagarose, (7) hydroxylapatite, (8) Superdex 200 (FPLC), (9) AX-300 (anion exchange, HPLC), (10) repeat AX-300, and (11) C-18 (reverse phase, HPLC). Chromatographic fractions were tested for the presence of the factor using the following assay: column fractions were mixed, 1:1 (v/v), with a solution containing ATP sulfurylase (1.0  $\mu\text{M}$ ), ATP (5.0 mM), [ $^{35}\text{S}$ ]SO $_4$  (0.50 mM, SA = 6.2 Ci/mol), MgCl $_2$  (6.0 mM), and inorganic pyrophosphatase (0.05 unit/ $\mu\text{L}$ ),  $T$  = 25 ( $\pm$  2)  $^\circ\text{C}$ . The products were separated and quantitated as described below. The preparation yielded approximately 6.3 mg of pure factor (0.06% of the extract protein).

**Cloning, Expression, Purification, and N-Terminal Sequencing of OASS.** OASS was cloned by PCR from an *E. coli* K-12 library using N- and C-terminal PCR primers constructed from the known OASS sequence. *Nde*I and *Bam*HI restriction sites were inserted at the 5' and 3' ends of the coding region. The sense and antisense primers were (5'-AAG GAC AGC ATA **TGA GTA** AGA TTT TTG) and (5'-AAC AAG **GGA TCC** TTA CTG TTG C), respectively (mismatched bases are shown in bold). The coding region was subcloned into the pET-23A expression vector. BL21-(DE3) containing the OASS expression plasmid was grown at 37  $^\circ\text{C}$  in LB medium containing ampicillin (50 mg/mL), pyridoxine (10  $\mu\text{M}$ ), and thiamin (15  $\mu\text{M}$ ). Expression of OASS was induced by adding IPTG (1.0 mM) 2 h prior to harvest. OASS was purified according to a published protocol (31) with the following exception: the anion-exchange step was replaced by a size exclusion chromatography step (Sephacryl S-300). This substitution obviates the need for extensive dialysis following ammonium sulfate precipitation. The resulting enzyme appeared pure by SDS-PAGE. The  $k_{\text{cat}}$  of the purified enzyme, 0.53 s $^{-1}$ , determined using the 5-thio-2-nitrobenzoate assay (32), was similar to that reported for the closely related enzyme from *Salmonella typhimurium*, 0.56 s $^{-1}$  (32). Approximately 50 mg of pure OASS was obtained per liter of cells. The N-terminus of OASS was sequenced, using the Edman degradation method, at the Laboratory for Macromolecular Analysis, Albert Einstein College of Medicine.

**Cloning, Expression, and Purification of Yeast APS Kinase.** The APS kinase coding region (*MET14*, accession no. 511138) was cloned from a yeast cDNA library by PCR using the following N- and C-terminal primers, respectively: 5'-GGGCCC**ATGGCT**ACTAATATTACTTGGC-3' and 5'-GGGCCT**CGAGCAA**TGCTTACGG-3'. The sequences in bold indicate *Nco*I and *Xho*I restriction sites used to insert the gene into the pET-28-a-c(+) expression plasmid (Novagen). The coding region was sequenced to ensure that it did not contain mutations. APS kinase was expressed in *E. coli* BL21-CodonPlus(DE3)-RIL by growing the cells to an OD $_{550}$  = 0.6 at 37  $^\circ\text{C}$ , temperature shifting to 18 ( $\pm$  2)  $^\circ\text{C}$ , adding IPTG (0.5 mM), and harvesting 18 h later. The cell pellet was suspended in Hepes/K $^+$  (50 mM, pH = 8.0), NaCl (300 mM), imidazole (5 mM), lysozyme (1 mg/mL), PMSF (0.50  $\mu\text{M}$ ), and pepstatin A (1.0  $\mu\text{M}$ ),  $T$  = 4 ( $\pm$  2)  $^\circ\text{C}$  and, 1 h later, sonicated. The sonicate was centrifuged at 15200 RCF for 1 h [4 ( $\pm$  3)  $^\circ\text{C}$ ]; the supernatant was collected and centrifuged again at 22500 RCF for 1 h [4 ( $\pm$  3)  $^\circ\text{C}$ ]. APS kinase was then affinity purified using an Ni-NTA column according to manufacturer's recommendations

(Qiagen) and purified further by size exclusion chromatography using a Superdex 200 resin equilibrated in Hepes/K<sup>+</sup> (50 mM, pH = 8.0). The resulting APS kinase appeared  $\geq 95\%$  pure by SDS-PAGE. The turnover number of APS kinase, measured using the pyruvate kinase lactate dehydrogenase detection system at APS (63  $\mu$ M), ATP (1.0 mM), MgCl<sub>2</sub> (2.0 mM), and Hepes/K<sup>+</sup> (50 mM, pH = 8.0), is 1.1 s<sup>-1</sup>.

**Figure 1: The ATP Synthesis Assay.** Coupled enzyme assays were initiated by the addition of 50  $\mu$ L of a given column fraction to 0.75 mL of an assay mixture containing Hepes/K<sup>+</sup> (50 mM, pH = 8.0), glucose (5.0 mM), NAD<sup>+</sup> (0.56 mM), MgCl<sub>2</sub> (5.2 mM), APS (0.20 mM), PP<sub>i</sub> (1.3 mM), hexokinase (0.34 milliunit/mL), and glucose-6-phosphate dehydrogenase (0.7 milliunit/mL). The progress of the reaction was followed by monitoring the reduction of NAD<sup>+</sup> to NADH at 340 nm. The recovery of activity after chromatography was assessed by comparing the total units of the cell extract with that of pooled fractions 31–44. The APS concentration was 0.50 mM; KCN (5.2 mM) and NaF (6.7 mM) were added to inhibit NADH oxidase and inorganic pyrophosphatase activities in the extract. All assays were performed at 25 ( $\pm 2$ ) °C and were linear with time and enzyme concentration.

**Figure 1: The APS Synthesis Assay.** The column fractions associated with the open circles were mixed 1:1 (v/v) with pooled fractions 31–34, and the resulting admixtures were assayed for APS synthesis activity. The reaction conditions were [<sup>35</sup>S]SO<sub>4</sub> (1.0 mM, SA = 4.7 Ci/mol), ATP/K<sup>+</sup> (23 mM), MgCl<sub>2</sub> (23 mM), APS kinase (0.2 unit/ $\mu$ L), and inorganic pyrophosphatase (0.05 unit/ $\mu$ L),  $T = 25 (\pm 2)$  °C. The activity recovered after chromatography was assessed by comparing the total activities of the cell extract and pooled fractions 46–55. The APS formed in these assays was completely converted to PAPS by the enzyme APS kinase. The reactions were quenched by boiling and centrifuged, and the supernatant was spotted onto a PEI–F TLC sheet. High concentrations of ATP were needed to maintain linearity in the cell extract assays. The radiolabeled reactants were separated on PEI–F TLC sheets using a 1.0 M LiCl mobile phase and quantitated using an AMBIS two-dimensional  $\beta$ -detector. The velocities were determined by linear fit of duplicate, four-point progress curves or, for the column fractions, at duplicate, single time point measurements. The assays are linear with time and enzyme concentration.

## RESULTS AND DISCUSSION

**Discovering the Pump.** The discovery of the metabolic pump began with the serendipitous observation that size exclusion chromatography of extracts containing plasmid-expressed ATP sulfurylase causes a 220-fold decrease in the total units of the forward reaction, while having no significant effect on the recovery of the reverse activity (see Figure 1). One hundred ten percent of the reverse activity in the extract applied to the size exclusion column was recovered in fractions 31–44 (●). These fractions contained the CysD and CysN subunits of ATP sulfurylase, and the peak of activity migrates at the apparent native molecular mass of ATP sulfurylase, 360 kDa. When these same fractions were assayed for the forward activity, they were found to contain 0.46% of the extract's activity (○). Thus, the metabolically relevant activity had decreased dramatically, while the

reverse activity remained unaffected. The lack of a significant effect on the reverse activity served as a control to indicate that the enzyme had not lost its intrinsic catalytic power but, rather, that the chromatography had separated a previously unknown "factor" from ATP sulfurylase that selectively affected the forward chemistry.

In an attempt to recover the lost activity, aliquots of the pooled ATP sulfurylase-containing fractions (i.e., 31–44) from the size exclusion column were mixed, in equal volume, with each remaining fraction, and the mixtures were assayed for the forward activity. A symmetric peak of recovered, forward activity was discovered, centered at 55 kDa (see Figure 1). The recovery of the forward activity was nearly complete: 80% of the extract's activity was recovered. The factor's ability to stimulate ATP sulfurylase was inactivated by treating the factor with protease, trypsin, or chymotrypsin or by heating at 65 °C for 5 min (see Materials and Methods). The inactivation results and apparent molecular mass of the factor suggested that it was a protein.

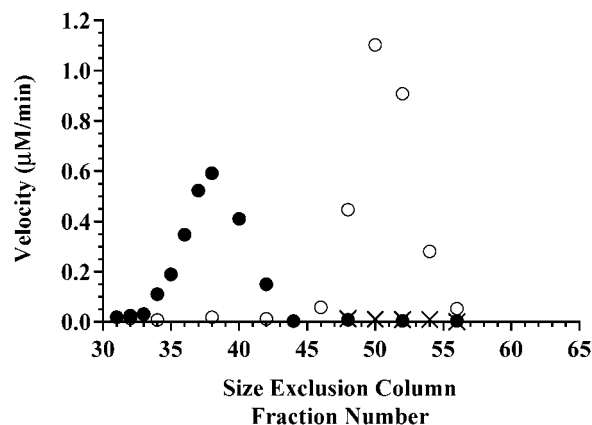


**FIGURE 1:** Discovering the pump pieces. Fractions from size exclusion chromatography of the cell extract were assayed for ATP (●) and APS (○) synthesis activity. 110% of the extract's ATP synthesis activity was recovered in fractions 31–44; however, these fractions contained only 0.46% of the extract's APS synthesis activity. Fractions 31–44 were pooled and mixed 1:1 (v/v) with each remaining fraction, and the admixtures were assayed for APS synthesis activity. 80% of the APS synthesis activity was recovered in fractions 46–55. Fractions 46–55 did not catalyze APS synthesis in the absence of the pooled fractions (×). The assay protocols are described in Materials and Methods.

**Purification and Identification of the Factor.** To obtain its N-terminal sequence, the factor had to be purified to homogeneity from wild-type levels in *E. coli* K-12. With the exception of size exclusion chromatography, the factor demonstrated 5–20-fold losses in specific activity over each of the matrices used in the purification. Reconstitution experiments, in which all of the fractions from a given chromatographic run were pooled, concentrated, and tested for ATP sulfurylase activation, did not recover the lost activity. Thus, the factor was inactivated in an unknown way by the chromatography. To overcome the losses in both protein and specific activity caused by the lengthy purification protocol, the purification began with an extract prepared from 180 L of wild-type cells. The cells were grown in a minimal salt medium in which sulfate is the sole source of sulfur, and *O*-acetyl-L-serine (the metabolic precursor of cysteine) was added to 1.0 mM at the onset of the last doubling of cells prior to harvest. These growth conditions



derepress expression of the cysteine regulon, which includes a minimum of 18 open reading frames (10) and upregulates levels of the cysteine biosynthetic enzymes ~250-fold (33). The purification required 11 chromatographic steps (see Materials and Methods). The last step of the purification, C-18 HPLC, yielded protein that appeared homogeneous by SDS-PAGE and was suitable for N-terminal sequencing.

The N-terminal sequence of the factor (SKIFEDNSLT) was determined (see Materials and Methods) and used as a query against the SwissProt database in the hope of finding a unique match to the N-terminus of a protein of known function. The single, perfect match to this sequence found in the database revealed that the factor was, in fact, the *A* (*aerobic*) isozyme of OASS (32), the last enzyme in the cysteine biosynthetic pathway. For the first time, it became clear that the entry of metabolites into this biosynthetic pathway was controlled by interactions between the enzymes that define its end points. N- and C-terminal primers, constructed from the OASS sequence, were used to clone OASS from an *E. coli* K-12 library by PCR. The enzyme was expressed in *E. coli* at high levels using the pET-23A vector. Overexpression allowed a simplification of the purification protocol (see Materials and Methods).

**OASS Binding Affects the Rate of APS Synthesis.** The very unfavorable energetics of APS and PP<sub>i</sub> formation prevents the detection of these products under typical experimental conditions. At 1.0 mM ATP and 0.25 mM SO<sub>4</sub> (the conditions associated with Figure 2), 0.02% conversion of substrate to product is predicted at equilibrium. Thus, detecting the forward reaction requires the addition of a thermodynamic bias in the forward direction, which can be achieved using the enzymes inorganic pyrophosphatase and APS kinase (together, their chemistries provide a  $-9$  kcal/mol bias). To determine whether the cloned, purified OASS alters the kinetic constants (and hence the mechanism) of the forward reaction catalyzed by the ATP sulfurylase from *E. coli*, its effects on the initial rate of the reaction were determined (Figure 2, panel A). The initial rate of APS and PP<sub>i</sub> synthesis in the presence of OASS, 0.53  $\mu$ M/min, is 440-fold greater than in its absence. The thermodynamic bias added in these experiments ensures that the observed effects derive solely from OASS-induced changes in the rate constants governing APS formation and that they are not due to a removal of product inhibition, since both products of the reaction are consumed by the coupling enzymes.

In the presence of a thermodynamic bias, OASS does not increase turnover of ATP sulfurylase from yeast (Figure 2, panel B). The primary sequence of the yeast enzyme is quite different from that of *E. coli*, and it lacks the GTPase subunit. Unlike its *E. coli* counterpart, the yeast ATP sulfurylase turns over readily in the presence of coupling enzymes. However, in the absence of the coupling enzymes, no product is detected either in the presence or in the absence of OASS. Thus, OASS does not act independently to create a thermodynamic bias on the forward reaction.

The effects of OASS were investigated further in a titration experiment in which the initial rate of APS synthesis was determined as a function of OASS concentration (Figure 2, panel C). The OASS-induced change in the initial rate of APS synthesis is saturable; at saturation, OASS stimulates the initial rate of APS synthesis  $1.6 \times 10^3$ -fold. The apparent dissociation constant for the ATP sulfurylase–OASS complex during

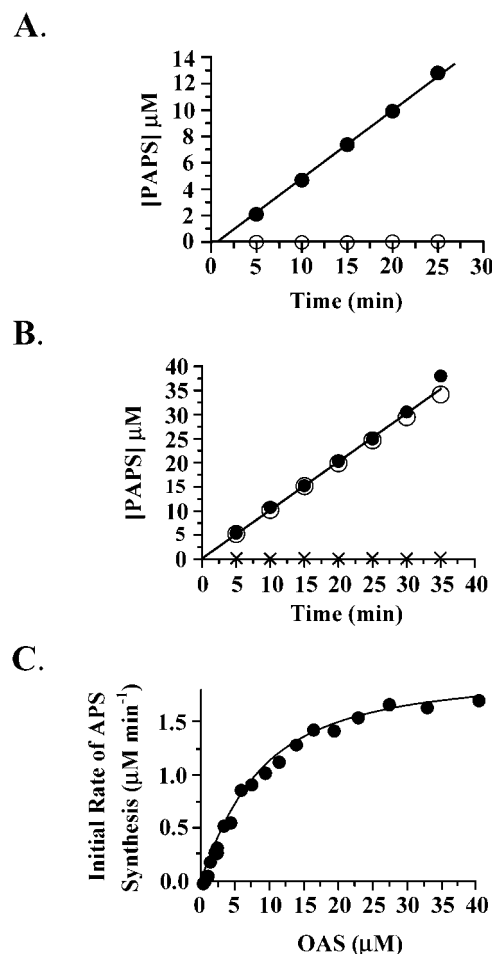


FIGURE 2: OASS affects the initial rate of APS synthesis. Panel A: OASS activates turnover of ATP sulfurylase from *E. coli*. The reaction conditions were *E. coli* ATP sulfurylase (1.0  $\mu$ M), OASS [0  $\mu$ M (○) or 40  $\mu$ M (●) active sites], inorganic pyrophosphatase (0.40 unit/mL), APS kinase (0.45 unit/mL), ATP (1.0 mM), [<sup>35</sup>S]-SO<sub>4</sub> (0.25 mM, SA = 0.46 mCi/mol), MgCl<sub>2</sub> (2.0 mM), Hepes/KOH (50 mM, pH = 8.0), and  $T = 25 (\pm 2)^\circ\text{C}$ . Panel B: OASS neither activates nor draws forward the reaction catalyzed by ATP sulfurylase from yeast. The reaction conditions were yeast ATP sulfurylase (1.0  $\mu$ M), OASS [0  $\mu$ M (○) or 40  $\mu$ M (● and ×) active sites], inorganic pyrophosphatase and APS kinase [0.40 and 0.45 unit/mL, respectively, or 0 unit/mL (×)]; the remaining conditions were identical to those described in panel A. Panel C: Titrating the effects of OASS. The reaction conditions were ATP sulfurylase (1.0  $\mu$ M), OASS (at the active site concentration indicated), ATP (1.0 mM), [<sup>35</sup>S]SO<sub>4</sub> (0.25 mM, 0.5 mCi/mmol), MgCl<sub>2</sub> (2.25 mM), Tris-HCl (50 mM, pH = 8.0), and  $T = 25 (\pm 2)^\circ\text{C}$ . Each of the data points in the three panels is the average of two to six measurements. All of the data were acquired in the initial rate phase of the reaction (i.e., less than 8% of the end point of the reaction had been reached). Radioactive reactants were separated using TLC and quantitated using a Molecular Dynamics detector.

initial rate turnover,  $K_A$ , is  $2.3 (\pm 0.3) \mu\text{M}$  (this value is for native OASS, a dimer). The alteration of kinetic constants of ATP sulfurylase by OASS and the well-behaved titration behavior strongly support the formation of an ATP sulfurylase–OASS complex.

**The ATP Sulfurylase–OASS Complex Couples ATP Hydrolysis and APS Synthesis.** In addition to its effects on the initial rate of APS synthesis, OASS profoundly affects the equilibrium position of the APS-forming reaction. The apparent equilibrium constant for the APS synthesis reaction, calculated from the plateau in the APS reaction progress

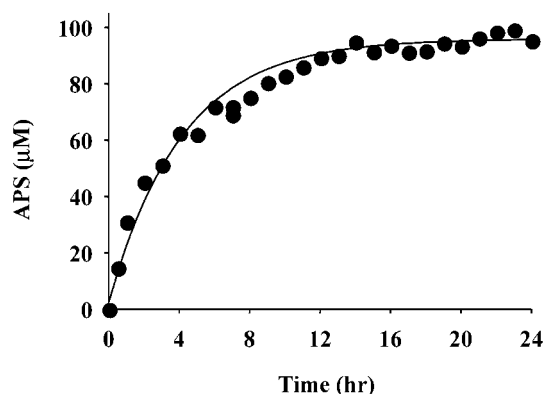


FIGURE 3: OASS affects the apparent equilibrium position of the APS reaction. The progress of the APS-forming reaction was monitored at a near-saturating concentration of OASS. The reaction solution contained ATP sulfurylase (5.0  $\mu$ M), ATP (1.0 mM), [ $^{35}$ S]-SO<sub>4</sub> (0.25 mM, 20  $\mu$ Ci/mmol), MgCl<sub>2</sub> (2.25 mM), OASS (30  $\mu$ M active sites, 5.5  $K_A$ ), and Tris-HCl (50 mM, pH = 8.0),  $T = 25 (\pm 2)^\circ\text{C}$ . Radiolabeled reactants were separated using TLC and quantitated using a Molecular Dynamics two-dimensional detection system. The apparent equilibrium constant, obtained from the plateau, is 0.083. This constant is  $3.5 \times 10^5$ -fold greater (i.e.,  $-7.5$  kcal/mol more favorable) than that observed in the absence of OASS.

curve at a saturating OASS concentration (Figure 3), is 0.083. The literature contains equilibrium constants for the APS synthesis reaction that vary from  $1.1 \times 10^{-8}$  to  $2.4 \times 10^{-7}$ . Using the more favorable equilibrium constant [ $2.4 \times 10^{-7}$  (35)], the value of 0.083 corresponds to a  $3.5 \times 10^5$ -fold increase, or a driving force of  $-7.5$  kcal/mol, which is approximately the free energy associated with the hydrolysis of the  $\beta,\gamma$ -bond of ATP. When this implication was pursued, we discovered that the ATP sulfurylase—OASS complex did, in fact, hydrolyze the  $\beta,\gamma$ -bond of ATP, using either  $\alpha$ - or  $\gamma$ -labeled ATP, and that the ratio of the initial rates of ATP hydrolysis and APS synthesis was 1.2:1.0 (Figure 4). ATP hydrolysis by the enzymes individually is quite low (i.e., less than 8% that of the complex under identical conditions).

The observed shift in the equilibrium constant for APS formation corresponds closely to the maximum free energy available to drive a reaction that is coupled to ATP hydrolysis with a stoichiometry of 1:1. Thus, the free-energy coupling efficiency of the system is quite high. Remarkably, new catalytic function, ATP hydrolysis, emerges from the interactions of these proteins, and the ATP hydrolysis and APS synthesis reactions are coupled through allosteric interactions that both accelerate catalytic turnover and couple the free energies of these two reactions.

**Distinct Sites for ATP and GTP Hydrolysis.** To assess whether the ATPase activity of the complex is due to an OASS-induced alteration of the ATP sulfurylase—GTPase active site that enables it to bind and hydrolyze ATP, GMPPNP was tested as an inhibitor, versus ATP, of the initial rate of APS synthesis. If the binding of ATP and GTP is mutually exclusive, a competitive inhibition pattern is expected. Alternatively, the nucleotides may bind at separate sites, in which case the results report the effects of the nucleotides and their interactions on the initial rate of APS synthesis. The results of the inhibition study were well fit, using the Cleland algorithm (36), to a linear noncompetitive model [i.e.,  $v = V_{\max}[A]/(K_M(1 + [I]/K_{IS})) + [A](1 + [I]/K_{II})$ , where  $K_I$  and  $K_{II}$  are the steady-state dissociation constants

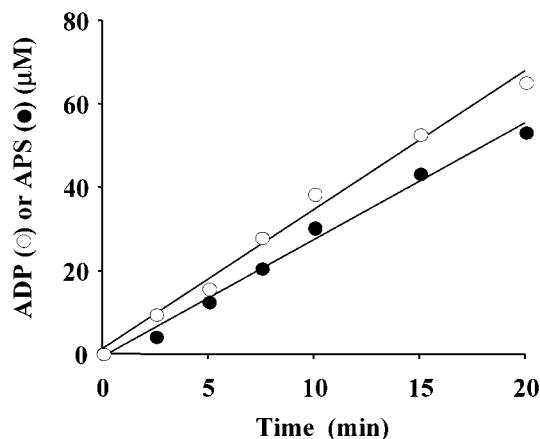


FIGURE 4: ATP hydrolysis:APS synthesis stoichiometry. The initial rates of ATP hydrolysis and APS synthesis were determined under identical conditions at a near-saturating concentration of OASS. The initial reaction rates were determined under the following conditions: ATP sulfurylase (5.0  $\mu$ M), [ $\alpha$ - $^{32}$ P]ATP (1.0 mM, 2.5  $\mu$ Ci/mmol), SO<sub>4</sub> (0.50 mM), MgCl<sub>2</sub> (2.5 mM), OASS (30  $\mu$ M active sites, 5.5  $K_A$ ), Tris-HCl (50 mM, pH = 8.0), and  $T = 25 (\pm 2)^\circ\text{C}$ . Radiolabeled reactants were separated using TLC and quantitated using a Molecular Dynamics two-dimensional detection system. The ATP hydrolysis reaction rate was corrected for the background ATP hydrolysis activity of the OASS [i.e.,  $7 (\pm 1)\%$  of the activity of the complex]. The ratio of the relative rates of ATP hydrolysis and APS synthesis is 1.2.

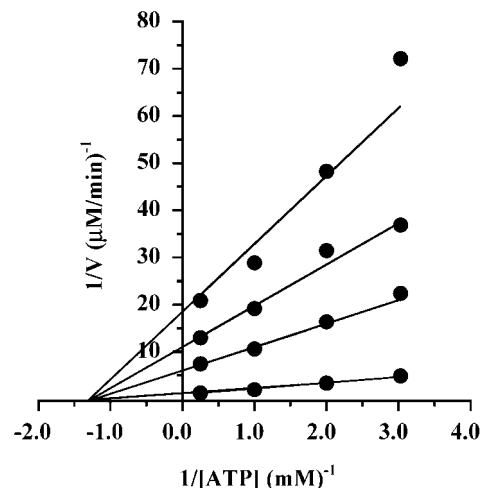


FIGURE 5: GMPPNP versus ATP inhibition of the OASS activation of ATP sulfurylase. The initial rate of APS synthesis was determined at the 16 conditions defined by a  $4 \times 4$  matrix of GMPPNP and ATP concentrations. Each point is the average of at least three determinations. In all cases, product formation was less than 7% of the reaction end point. The conditions were ATP sulfurylase (1.25  $\mu$ M), OASS (40  $\mu$ M active sites,  $7.3 \times K_A$ ), [ $^{35}$ S]-SO<sub>4</sub> (0.25 mM, SA = 0.46 mCi/mol), ATP (4.0, 1.0, 0.5, 0.33 mM), GMPPNP (0, 0.10, 0.20, 0.35 mM), MgCl<sub>2</sub> ([ATP] + [GMPPNP] + 1.0 mM), Tris-HCl (50 mM, pH = 8.0), and  $T = 25 (\pm 2)^\circ\text{C}$ . Radiolabeled reactants were separated using TLC and quantitated using a Molecular Dynamics detection system.

of GMPPNP with and without ATP bound, respectively]. The noncompetitive behavior reveals that the complex contains a separate binding site for each ATP and GMPPNP, and the intersection of the set of  $1/v$  vs  $1/[ATP]$  lines on the  $1/[ATP]$  axis indicates that the steady-state affinity of a given active site for its nucleotide is not influenced by occupancy at the other site [i.e.,  $K_I$  (33 ( $\pm 3$ )  $\mu$ M)  $\sim K_{II}$  (28 ( $\pm 1.8$ )  $\mu$ M)]. The inhibition constant for the binding of GMPPNP to the E·ATP·SO<sub>4</sub> complex of ATP sulfurylase (in the

absence of OASS) is  $29 (\pm 5) \mu\text{M}$  (37), which, when compared to  $K_I$  and  $K_{II}$ , suggests that its affinity is affected only slightly, if at all, by the binding of OASS. Taken together, the information suggests, but does not prove, that the system is capable of assembling its full complement of nucleotides and substrates and proceeding forward into its reaction coordinate to an as yet undetermined stage, at which point the forward catalysis is stalled by the inability to hydrolyze the  $\beta, \gamma$ -bond of GTP.

## CONCLUSIONS

The formation of functional hierarchies from the interactions of cellular constituents is an important and somewhat elusive property of the cellular matrix. The cysteine biosynthetic pump demonstrates well how known constituents can combine in unexpected ways to produce "new" function. In this case, the *new* function is catalytic, and it controls the steps of the process (cysteine biosynthesis) that are carried out by the elements whose interactions are required to produce it. In this context, it is worth noting that APS kinase, the second enzyme in the cysteine biosynthetic pathway, is appended to the C-terminus of the GTPase subunit of many Gram-negative ATP sulfurylases. APS kinase phosphorylates the 3'-hydroxyl of APS. Moreover, OASS forms a tight complex with its predecessor in the pathway, serine transacetylase (38, 39), which transfers the acetyl group from acetyl-CoA to L-serine to form *O*-acetyl-L-serine. These facts suggest that the enzymes of the pathway might organize into a yet higher order complex. These issues are currently under investigation in this laboratory. The fact that an ATPase-driven energy pump can be constructed out of the allosteric interactions of cysteine biosynthetic enzymes suggests that such energy-coupled systems may occur elsewhere in metabolism and raises the ever-intriguing issue of how the cell creates hierarchies of function from the synergism inherent in the organization of its matrix.

## REFERENCES

- Sablin, E. P., Kull, F. J., Cooke, R., Vale, R. D., and Fletterick, R. J. (1996) *Nature* 380, 555–559.
- Vale, R. D., and Milligan, R. A. (2000) *Science* 288, 88–95.
- Rayment, I., Holden, H. M., Whittaker, M., Yohn, C. B., Lorenz, M., Holmes, K. C., and Milligan, R. A. (1993) *Science* 261, 58–65.
- Abrahams, J. P., Leslie, A. G., Lutter, R., and Walker, J. E. (1994) *Nature* 370, 621–628.
- Bianchet, M. A., Hullihen, J., Pedersen, P. L., and Amzel, L. M. (1998) *Proc. Natl. Acad. Sci. U.S.A.* 95, 11065–11070.
- Rastogi, V. K., and Girvin, M. E. (1999) *Nature* 402, 263–268.
- Jencks, W. P. (1997) *Annu. Rev. Biochem.* 66, 1–18.
- Jencks, W. P. (1989) *Methods Enzymol.* 171, 145–164.
- Frey, P. A., and Arabshahi, A. (1995) *Biochemistry* 34, 11307–11310.
- Leyh, T. S. (1993) *Crit. Rev. Biochem. Mol. Biol.* 28, 515–542.
- Kreditch, N. M. (1987) in *Escherichia coli and Salmonella typhimurium* (Neidhardt, F. C., Ed.) Vol. 1, pp 419–428, American Society of Microbiology, Washington, DC.
- Liu, C., Martin, E., and Leyh, T. S. (1994) *Biochemistry* 33, 2042–2047.
- Wei, J., and Leyh, T. S. (1999) *Biochemistry* 38, 6311–6316.
- Peck, H. D., Jr. (1993) in *The Sulfate-Reducing Bacteria: Contemporary Perspectives* (Odom, J. M., and R. S., Jr., Eds.) pp 41–75, Springer-Verlag, New York.
- Falany, C. N., Wheeler, J., Oh, T. S., and Falany, J. L. (1994) *J. Steroid Biochem. Mol. Biol.* 48, 369–375.
- Pasqualini, J. R., Schatz, B., Varin, C., and Nguyen, B. L. (1992) *J. Steroid Biochem. Mol. Biol.* 41, 323–329.
- Brand, S. J., Andersen, B. N., and Rehfeld, J. F. (1984) *Nature* 309, 456–458.
- Roth, J. R., and Rivette, A. J. (1982) *Biochem. Pharmacol.* 31, 3017–3021.
- Hemmerich, S., Bertozzi, C. R., Leffler, H., and Rosen, S. D. (1994) *Biochemistry* 33, 4820–4829.
- Ishihara, M., Guo, Y., and Swiedler, S. J. (1993) *Glycobiology* 3, 83–88.
- Tai, C. H., and Cook, P. F. (2000) *Adv. Enzymol. Relat. Areas Mol. Biol.* 74, 185–234.
- Burkhard, P., Rao, G. S., Hohenester, E., Schnackerz, K. D., Cook, P. F., and Jansonius, J. N. (1998) *J. Mol. Biol.* 283, 121–133.
- Satishchandran, C., and Markham, G. D. (1989) *J. Biol. Chem.* 264, 15012–15021.
- Baddiley, J., Buchanan, J. G., and Lett, R. (1957) *J. Chem. Soc.*, 1067–1071.
- Vieira, J., and Messing, J. (1982) *Gene* 19, 259–268.
- Leyh, T. S., Taylor, J. C., and Markham, G. D. (1988) *J. Biol. Chem.* 263, 2409–2416.
- Tabor, S., and Richardson, C. C. (1985) *Proc. Natl. Acad. Sci. U.S.A.* 82, 1074–1078.
- Vogel, H. J., and Bonner, D. M. (1956) *J. Biol. Chem.* 218, 97–106.
- Ostrowski, J., and Kredich, N. M. (1991) *J. Bacteriol.* 173, 2212–2218.
- Bachmann, B. J. (1996) in *Escherichia coli and Salmonella typhimurium: Cellular and Molecular Biology* (Neidhardt, F. C., et al., Eds.) Vol. II, pp 2460–2488, American Society for Microbiology, Washington, DC.
- Hara, S., Payne, M. A., Schnackerz, K. D., and Cook, P. F. (1990) *Protein Expression Purif.* 1, 70–76.
- Tai, C. H., Nalabolu, S. R., Jacobson, T. M., Minter, D. E., and Cook, P. F. (1993) *Biochemistry* 32, 6433–6442.
- Ellis, R. J., Humphries, S. K., and Pasternak, C. A. (1964) *Biochem. J.* 92, 167–172.
- Flodgaard, H., and Fleron, P. (1974) *J. Biol. Chem.* 249, 3465–3474.
- Foster, B. A., Thomas, S. M., Mahr, J. A., Renosto, F., Patel, H. C., and Segel, I. H. (1994) *J. Biol. Chem.* 269, 19777–19786.
- Cleland, W. W. (1979) *Methods Enzymol.* 63, 103–138.
- Liu, C., Suo, Y., and Leyh, T. S. (1994) *Biochemistry* 33, 7309–7314.
- Cook, P. F., and Wedding, R. T. (1978) *J. Biol. Chem.* 253, 7874–7879.
- Kredich, N. M., Becker, M. A., and Tomkins, G. M. (1969) *J. Biol. Chem.* 244, 2428–2439.

BI025953J